PREPARED FOR
ELECTRIC RELIABILTY COUNCIL OF TEXAS

SIMULATION OF WIND GENERATION PATTERNS FOR THE ERCOT SERVICE AREA

MAY 23, 2012

SUBMITTED BY:
AWS Truepower, LLC
Kenneth Pennock, Forecasting and Research Business Manager
463 New Karner Road
Albany, NY 12205
kpennock@awstruepower.com
Tel: 518-213-0044 ext. 1075

AWS Truepower™
Where science delivers performance.

TABLE OF CONTENTS

LIST OF FIGURES

LIST OF TABLES

1. INTRODUCTION

In January 2012, AWS Truepower (AWST) was engaged by the Electric Reliability Council of Texas (ERCOT) to provide 15 years of wind power data for existing, planned, and hypothetical sites. These data were to be based on high-resolution simulations of the historical climate performed by a mesoscale numerical weather prediction (NWP) model covering the period 1997 through 2011.

The work was divided into the following technical tasks:

1. Generate historical wind and weather data for the ERCOT service area.
2. Work with ERCOT to compile a representative list of existing and proposed project sites and identify hypothetical sites for new wind projects in the service area.
3. Convert wind and weather data to power output.
4. Package and deliver time series of 15 years of power output at each site.
5. Compile results and report on findings.

Several assumptions have been made in order to facilitate the delivery of the requested data sets. These assumptions were proposed by AWST and then applied based on ERCOT's recommendations. This document presents AWST's final technical report on the methods used, the results achieved, and a validation of the data sets.

2. PREVIOUS ERCOT PROJECTS

AWST has previously performed similar studies for ERCOT. This study expands upon the previous work by increasing the study period and providing output for individual sites. The first study identified Competitive Renewable Energy Zones (CREZs) and characterized hourly, daily, and seasonal output of existing and future wind projects in proposed CREZs to enable assessment of potential transmission upgrades.[1] A summary of the steps used in that study are as follows:

- Created hourly output for a typical year (sampled from 1990-2004)
- Used Texas MesoMap for map adjustment and hourly wind speeds (validated with 64 towers)
- Employed site screening
- Total of 1200 sites (13 GW) covering each region of Texas
- Each site was at least 100 MW and above a specified minimum net capacity factor
- Identified 25 Competitive Renewable Energy Zones (CREZs)
- Output was provided for 4000 MW of capacity in each CREZ (not individual sites)

A subsequent study used the CREZs selected from the first study to produce model-derived wind plant output and forecast data for two continuous years. [2] Details are summarized as follows:

- Generated hourly and 1-minute plant output, 4 hour ahead and next day hourly forecasts
- Modeled hourly 80-m wind speeds for 2005–2006 (10 km resolution)

[1] AWS Truewind, LLC, "Wind Generation Assessment", Report to ERCOT, January 2007.

[2] AWS Truewind, LLC, "Wind Generation and Forecasting Profiles", Report to GE Energy Consulting, October 2007.

- Converted to power output
- 716 sites in 25 CREZs from previous study
- Provided output for each site so different scenarios within each CREZ could be tested
- Locations of sites were not provided, but location of CREZs were

The current study employs similar methodology as the most recent work but extends the time period from two years to 15 years of hourly simulated data. Additionally, power profiles were delivered for individual sites rather than aggregated to each CREZ.

3. SITE SELECTION

AWST worked with ERCOT to identify existing, proposed (queue), and hypothetical sites, with the aim of generating over 25 GW of onshore sites. ERCOT also requested offshore sites totaling 1500 MW.

The site selection process operated in four distinct phases. The first phase identified the existing wind plants in the ERCOT service area. ERCOT provided AWST with a list of existing and queue wind plants. This list included the approximate location and capacity of each site. AWS Truepower then gathered mean wind speed and elevation data for each wind farm by digitizing the wind turbine occupied area in a GIS software package. Figure 1 shows an example of a wind farm digitized from individual turbine locations. The wind turbine locations were provided by AWS Truepower's Wind Farm and Turbine Inventory database (WFTI). The AWST WFTI is compiled from the Federal Aviation Administration public record of tall towers and aerial imagery from Landsat.

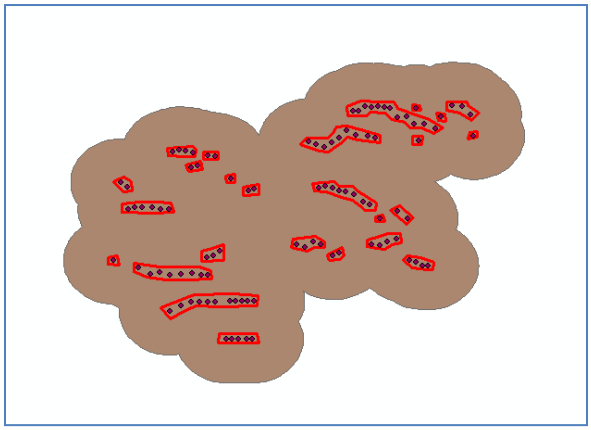

Figure 1. Example of an existing wind farm digitized (red polygons) for use in this study. The brown area indicates a 2-km buffer around each turbine identified from the WFTI database. Individual turbines are indicated in black.

The second phase identified queue sites in a different manner. AWST ran GIS-based site selection software to build sites based on wind resource and excluded areas within a range of the approximate locations provided by ERCOT. To provide a consistent set of resource estimates for ranking and selecting sites, a seamless map of predicted mean wind speeds at 80 m for the ERCOT region was prepared from AWS Truepower's proprietary wind maps. This map was generated at a horizontal resolution of 200 m which is sufficiently fine to reflect the influence of most terrain features and to identify specific locations for wind projects. AWS Truepower has developed a method of adjusting its wind maps using a wide

array of wind resource measurements to ensure good accuracy.[3] A map of the estimated net capacity factor for a composite International Electrotechnical Commission (IEC) Class 2 wind turbine[4] was then created using the seamless wind speed map at 80 m and speed-frequency distributions compiled from 15 years of historical mesoscale model runs (a total of 366 randomly sampled days) previously performed by AWS Truepower at 10 km resolution. Although IEC Class 2 turbines are not suitable for every site, the use of a single power curve allowed for an objective ranking of resource potential. The composite power curve was created by taking the average of three commercial megawatt-class wind turbine power curves which had been normalized to their rated capacity. The composite curve is shown in Table 1.

Table 1. Composite power curves.

Speed	IEC - 1	IEC - 2	IEC - 3	Offshore
0	0	0	0	0
1	0	0	0	0
2	0	0	0	0
3	0	0	0.0063	0
4	0.0195	0.0283	0.0412	0.0252
5	0.0681	0.0884	0.102	0.0704
6	0.1401	0.1739	0.189	0.1296
7	0.2371	0.2873	0.3107	0.2162
8	0.3663	0.4339	0.4715	0.3276
9	0.5233	0.6066	0.6629	0.4670
10	0.7021	0.7768	0.8383	0.6340
11	0.8564	0.905	0.9464	0.8034
12	0.9556	0.9717	0.9871	0.9510
13	0.9874	0.9926	0.9976	1
14	0.9945	0.9979	0.9995	1
15	0.9982	0.9998	0.9999	1
16	0.999	1	1	1
17	1	1	1	1
18	1	1	1	1
19	1	1	1	1
20	1	1	1	1
21	1	1	1	1
22	1	1	0	1
23	1	1	0	1
24	1	1	0	1
25	1	1	0	1

The site screening took into account the following areas excluded from development:

- From the United States Geological Survey National Land Cover Database (2001):

[3] The mean bias of the AWS Truepower 200-m USA wind map is found to be virtually zero, while the standard error (after accounting for uncertainty in the data) is 0.35 m/s.

[4] IEC Class 2 turbines are typically used for sites with 7.5–8.5 m/s average wind speeds at hub height.

- Open water
- 200-m buffer of developed low intensity
- 500-m buffer of developed medium intensity
- 500-m buffer of developed high intensity
- Woody wetlands
- Emergent herbaceous wetland

- From the Environmental Systems Research Institute database:
  - Parks
  - Parks detailed
  - Federal lands (non-public)
  - 10,000-ft. buffer of small airports (all hub sizes)
  - 20,000-ft. buffer of large airports (hub sizes medium and large)
- Other:
  - Slopes greater than 20%
  - Areas outside the study region
  - Areas of natural and scientific interest (ANSI)
  - -2km buffer around existing wind farms

Based on the net capacity factor map, areas excluded from development, and the queue site capacities and approximate locations, the site selection software finds all sites with the desired output in the immediate vicinity (i.e., a local maximum) with sufficient area to support a project of the desired rated capacity. The software reviews the candidate sites and retains the site with the highest capacity factor, dropping the other sites. This process is conceptualized in Figure 2.

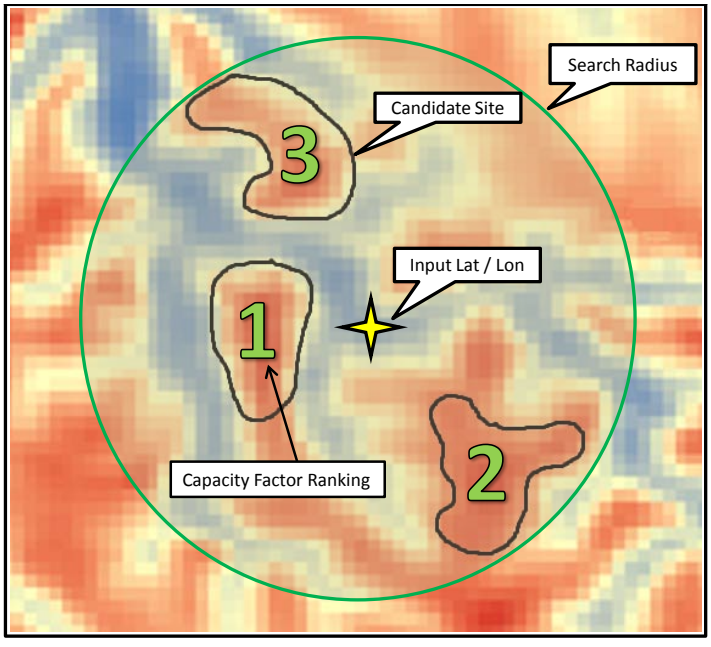

Figure 2. A conceptual depiction of the site selection process. Cool colors indicate lower capacity factor values.

Once the existing and queue wind plants were identified, the third site selection phase identified hypothetical sites. A 2-km buffer around each identified existing and queue site was created and added to areas excluded from development to ensure unique hypothetical sites. A similar site selection algorithm was then employed, with the exception that instead of supplying approximate locations, capacities, and search radii, the algorithm determines likely locations of hypothetical sites within a specified range of capacities based on the available wind resource. The screening for hypothetical sites employs two steps. In the first step, the program finds all sites with a maximum output in the immediate vicinity as before. In the second step, the program allows each of these sites to expand so long as the output does not decrease by more than 5%. If the site encounters another site, the site that has a higher mean output is retained and the other is dropped. The program was run in an iterative process until the nameplate capacity target by county was reached.

A fourth phase of site selection identified 3 offshore sites totaling 1500 MW. ERCOT provided AWS Truepower a list of three counties in Texas where nearby offshore wind development is expected. AWS constructed three 500 MW plants (one for each nearby county) in the offshore area waters. These sites were placed in areas that were least 5 miles from shore and in waters less than 30 m deep. No other restrictions on offshore development were applied. For each offshore development region, AWS Truepower selected an area with the greatest expected capacity factor that could support 500 MW of wind development.

Figure 4 shows the locations of existing, queue, and hypothetical sites overlaid on the average annual capacity factor map at 80 m above ground level. The sites are summarized in Table 2, while Appendix A contains the final list of 228 sites approved by ERCOT for use in this study.

Table 2. Summary of sites used in the study including the total number of each type and total GW of power selected.

PLANT TYPE	NUMBER	GW
Existing Sites	84	9.9
Queue Sites	11	1.9
Hypothetical Sites	130	17.9
Offshore Sites	3	1.5
Total	228	31.2

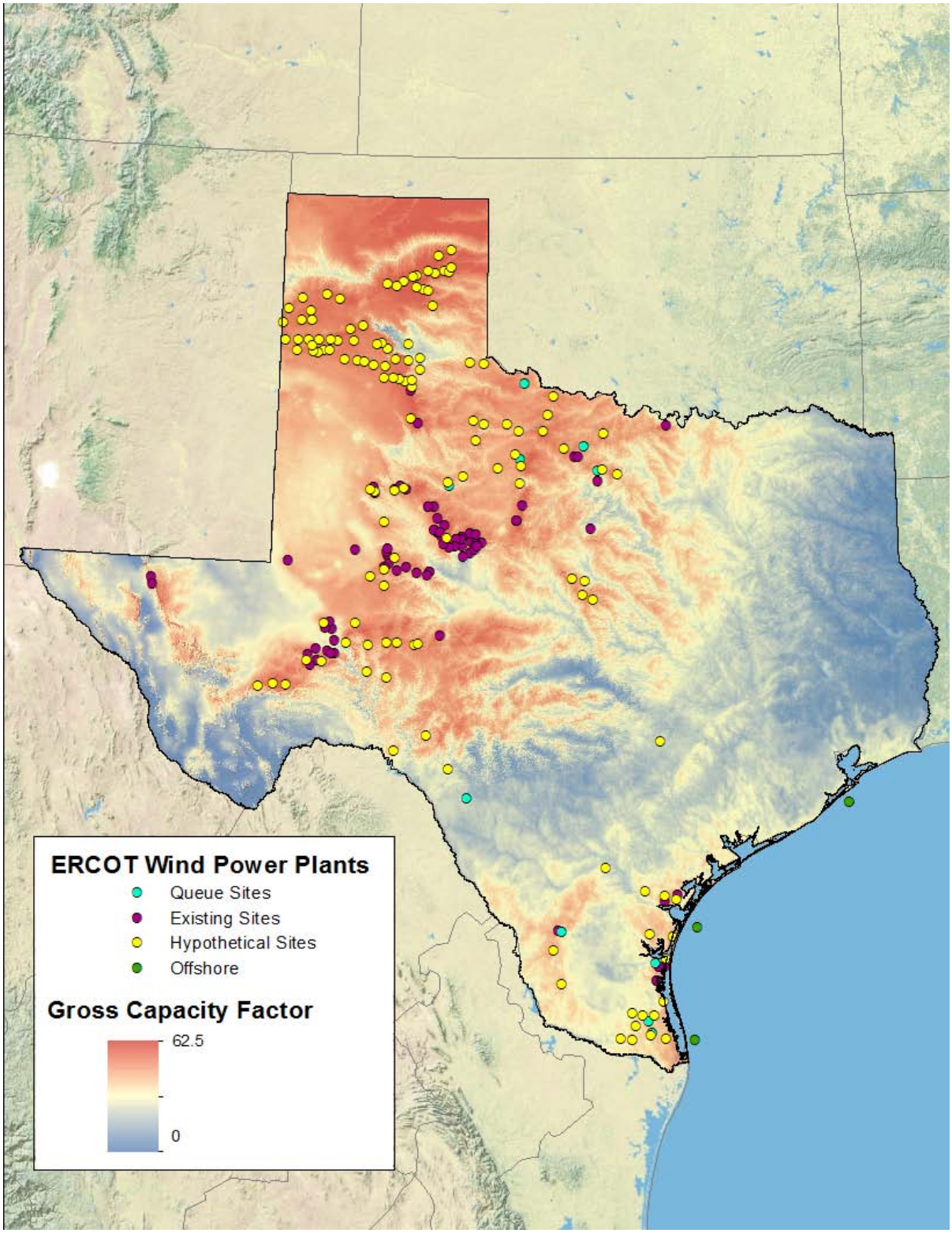

Figure 3. Annual capacity factor map at 80-m hub height and locations of all sites in the study. Each site type is identified by different color circles.

4. MESOSCALE MODELING

Meteorological data used to produce wind power output profiles at each selected site was generated with the Mesoscale Atmospheric Simulation System (MASS), a proprietary numerical weather prediction model developed by AWST partner MESO, Inc.[5] MASS is a non-hydrostatic weather model which has been customized for near-surface wind and irradiance prediction. MASS simulates the fundamental physics of the atmosphere including conservation of mass, momentum, and energy as well as the moisture phases using a variety of online, global, geophysical and meteorological databases. The main meteorological inputs are reanalysis data, rawinsonde data, and land surface measurements. The reanalysis database – the most important – is a gridded historical data set produced by the U.S. National Centers for Environmental Prediction and National Center for Atmospheric Research (NCEP/NCAR Reanalysis; NNGR). The data provide a snapshot of atmospheric conditions around the world at all levels of the atmosphere in intervals of six hours. Along with rawinsonde and surface data, the reanalysis data establish the initial and lateral boundary conditions for the MASS runs. The MASS model itself determines the evolution of atmospheric conditions within the region based on the interactions among different elements in the atmosphere and between the atmosphere and the surface.

The reanalysis data are on a relatively coarse grid (about 210-km spacing). To avoid generating noise at the boundaries that can result from large jumps in grid cell size, mesoscale models such as MASS are typically run using nested grids of successfully finer mesh size until the desired grid scale is reached. In this configuration, the outer grid provides initial guess fields and updated lateral boundary conditions for each subsequent nest of an inner grid. For this study, a nested grid scheme with horizontal resolutions of 30 km and 8 km was used (Figure 4). The runs cover Texas and it's offshore for the period 1 January 1997 to 1 January 2012. Table 3 summarizes the model configuration used in this study.

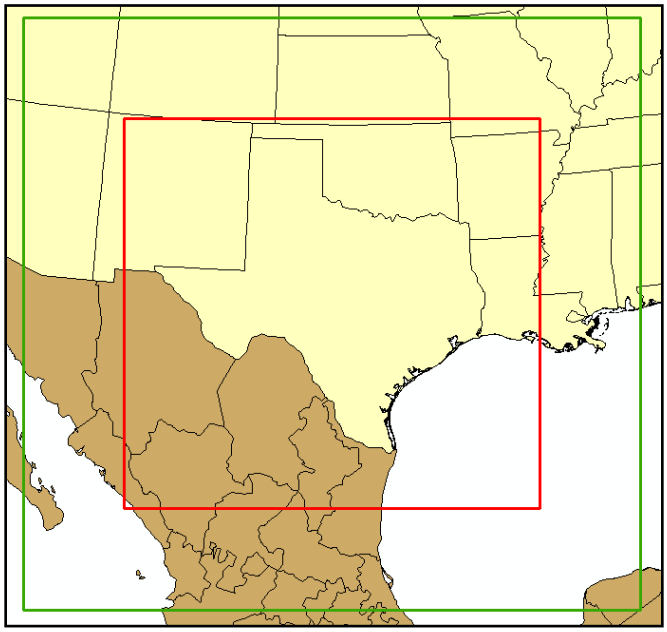

Figure 4. ERCOT study area and proposed mesoscale model configuration. The model configuration includes nested grids of 30-km (green) and 8-km (red) grid spacing.

[5]Manobianco, J., J. W. Zack, and G.E. Taylor, 1996: Workstation-based real-time mesoscale modeling designed for weather support to operations at the Kennedy Space Center and Cape Canaveral Air Station. Bull. Amer. Meteor. Soc., 77, 653-672. Available online at http://science.ksc.nasa.gov/amu/journals/bams-1996.pdf.

Table 3. Model configuration for MASS runs.

Model	MASS v. 6.8
Initialization data source	NNGR
Data assimilated in the course of simulations	Rawinsonde, surface observations (temperature, dew point, wind direction and speed, pressure)
Sea-surface temperatures	MODIS (Moderate Resolution Imaging Spectroradiometer)
Cumulus scheme	Kain-Fritsch
Spin-up	12 hours before start of valid run
Length of run	15-16 day series (e.g., Jan 1-15, Jan 16-31)
Frequency of data sampling	Hourly
Data stored	Wind speed and direction, temperature, pressure, TKE at five heights; surface temperature and pressure, specific humidity, incoming long-wave and short-wave radiation, precipitation

5. GENERATION OF WIND PLANT OUTPUT

An algorithm written by AWST was used to convert the meteorological data generated by the mesoscale model to wind plant output. The software starts by reading a list of seven tall towers[6] in the validation region and their nearest associated grid cells (grid number and column and row position). It also reads a list of the grid cells associated with the sites. Up to eight 8-km grid cells are associated with each site, depending on its size and shape and if it falls along the boundary of grid cells. For each cell, the list provides the latitude and longitude, expected mean speed of the part occupied by turbines, mesoscale grid cell elevation, actual mean elevation of the turbines, and relative proportion of the site's total rated capacity associated with that cell. The mean speeds are based on AWS Truepower's 200-m resolution wind map. An example of 200-m map grid cells within four 8-km model grid cells for a hypothetical site is shown in Figure 5.

[6] The location of the tall towers is proprietary, and therefore not disclosed in this report.

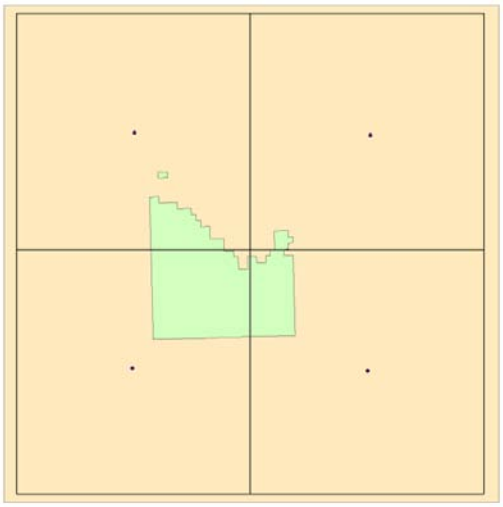

Figure 5. Example of 200-m map cells within 8-km model grid cells for a hypothetical site.

The program then imports the turbine power curves. The appropriate power curve was applied at each site, reflecting the estimated IEC site classification. A composite power curve was created from commercially available turbines for each IEC class (see Table 1). The power curves are scaled to a rated capacity of 2 MW and are valid for the standard sea-level air density of 1.225 kg/m^3. The IEC 1 and 2 turbines are assumed to have a hub height of 80 m and the IEC 3 turbine 100 m. It is assumed that the lower hub height will be used unless the wind resource dictates moving to a higher hub height to capture more wind. The program next reads a set of 12x24 speed matrixes, one for each of the validation towers. These matrixes give the mean speed for each hour of the day and for each month of the year. For each tower there are two matrices, one for each hub height (80 m and 100 m).[7] The program reads the mesoscale time series file for each of the grid points nearest the validation towers. From the wind speed data, it creates a 12x24 mean speed matrix for each hub height. The ratio between the average observed and average simulated speed is then calculated for each bin and normalized to an average of one. The result is an adjustment matrix which is used to correct model biases. Although the program calculates adjustments on a monthly basis, it was found during the validation phase that the monthly variation in speeds was accurately predicted by the model. Therefore, only an annual adjustment is performed.

The mesoscale time series files are then read for each grid cell associated with a project site. The speed data are scaled to match the expected mean speed and finally summed for all the grid cells associated with the site. In the sum, each cell's speeds are weighted according to the proportion of the site area associated with that cell. The result is a time series of simulated wind speeds for the site as a whole at both 80 m and 100 m.

The program calculates a correlation coefficient (r^2) between the simulated daily mean speeds for the site in question and the simulated daily mean speeds for each validation location. It then calculates a weighted average adjustment matrix for the site in which the weight given to the adjustment matrix for each validation location is proportional to its correlation coefficient. The program applies this blended

[7] The matrices were created from the tall tower observations, smoothed with data from long-term reference stations where necessary. In cases where the monitoring height was lower than the modeled hub heights, the diurnal shear distribution was used to extrapolate to 80 and 100 m.

adjustment matrix to the simulated data for the site. For example, if the time in question is 1300, the simulated speed is multiplied by the adjustment factor for 1300.

The speed at each grid point is then adjusted for wake losses in a manner that depends on the simulated wind direction relative to the prevailing (most frequent) direction. The loss is given by $w = w_{\min} + (w_{\max} - w_{\min})\sin^2(\theta - \theta_{\max})$, where $w_{\min}$ is the minimum loss (assumed to be 4%) when the wind is aligned with or opposite to the prevailing direction $\vartheta_{\max}$, and $w_{\max}$ is the maximum loss (9%) when the wind is perpendicular to the prevailing direction. The loss factors account both for wake losses and implicitly for other losses such as blade soiling that affect the efficiency of power conversion for a given free-stream speed without reducing the maximum output. These losses were determined by trial and error to conform to AWS Truepower's estimates for actual wind projects. The method does not account for sites where there is more than one prevailing wind direction or where the prevailing energy-producing direction differs from the most frequent direction. In these cases, only the most prevalent wind direction is used.

The speed is further adjusted by adding a random factor (from -1 to +1) multiplied by the predicted TKE. This adjustment is intended to reflect the impact of gusts on the speeds experienced by the turbines in the wind project. The frequency and intensity of such simulated gusts depends to a degree on time of day, as TKE is generally higher in the day when the planetary boundary layer is thermally unstable or neutral than at night when it is thermally stable.

The program selects the most appropriate IEC class based on the estimated maximum long-term annual mean speed within the site based on the ERCOT wind map, adjusted for air density. The program then applies an additional power loss to account for turbine and plant availability. Based on data obtained by AWS Truepower for operating wind projects, the availability is assumed to follow a normal distribution with a mean of 94.8% and a standard deviation of 2.3%; the distribution is truncated at 100%. To avoid unrealistic rapid fluctuations in output, the availability is allowed to change at random intervals averaging only once per hour. An additional loss of 3% is subtracted from the output to represent electrical losses.

The resulting output at each site is then adjusted to reduce the impact of observations assimilated into the mesoscale model every 12 hours. This adjustment removes a small correlated component of the variability from each site, resulting in a more realistic, consistent diurnal variability when all simulated sites are aggregated across the system.

A 15-year time series of hourly power output was created at each site. A sample text file of site output is shown in Table 4. The header includes the site number, rated capacity, and IEC class of the site, along with the wind speed level used in the calculations and the resulting average loss applied at the site. ERCOT requested the data be reformatted into yearly files that included all sites as shown in Table 5, with all times in local time (Central Standard Time, CST) rather than Greenwich Mean Time (GMT) as was provided in the original site files.

Table 4. Sample plant output data file

SITE NUMBER:		1
CAPACITY (MW):		757
IEC CLASS:		1
WIND SPEED LEVEL (M):		80
AVERAGE LOSS (%):		16.86
YYYYMMDD	**HHMM(GMT)**	**OUTPUT(MW)**
19970101	0000	366.9
19970101	0100	326.2
19970101	0200	291.1
19970101	0300	378.7
19970101	0400	417.5
19970101	0500	492.1
19970101	0600	574.4
19970101	0700	497.3

Table 5. Sample yearly data file.

YYYYMMDD	HHMM (CST)	SITE_00001: capacity= 112.5	SITE_00002: capacity= 77.2	SITE_…	SITE_20003: capacity= 500.0
19970101	1900	80.37	5.07	…	127.26
19970101	2000	70.94	3.39	…	133.47
19970101	2100	51.89	3.51	…	146.3
19970101	2200	44.81	11.04	…	218.41
19970101	2300	33.19	61.91	…	215.01

6. VALIDATION

The delivered data sets underwent a detailed validation process to ensure the results were consistent with actual meteorological and power generation observations. AWST used as much publicly and privately available observed data as possible at the time of the study. This included nine National Weather Service Automatic Surface Observing System (ASOS) stations, seven proprietary tall tower measurements, and wind power output from 10 ERCOT generation facilities. Each of these data sources was independently validated against the modeled data to determine the accuracy of the provided data sets.

ASOS winds are measured at a standard 10-m height. Nine stations across Texas were used to compare winds from the MASS model runs at 10 m. Figure 6 demonstrates the results from this analysis, showing two of the ASOS stations (Abilene and Port Isabel Cameron) and the nearest corresponding modeled grid point. The plots compare the deviation from the long term average wind speed and show the monthly 10 m correlation coefficient between the ASOS and modeled locations. The interannual variability of the simulated wind speed compares well with the observed wind speed at all nine

locations, with the model trending particularly close to the observations on a monthly basis with an average correlation coefficient of 0.743.

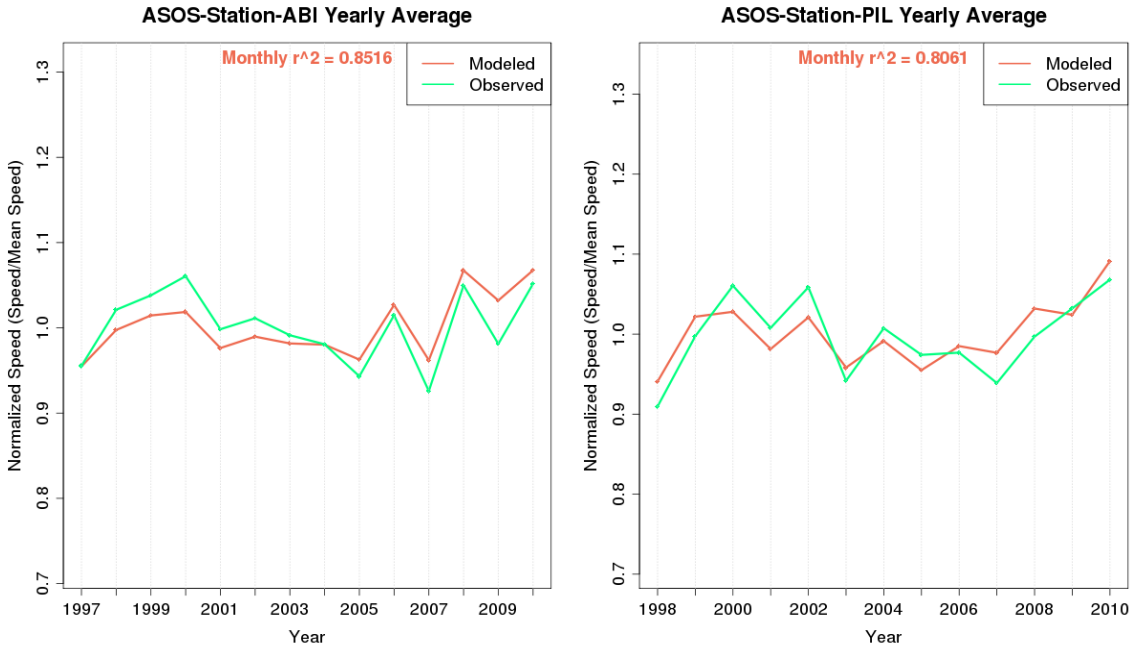

Figure 6. Comparison of the long term modeled wind speed at two ASOS stations in the ERCOT region.

The modeled 80-m wind speeds were compared to wind speeds measured at seven validation towers and sheared to 80 m by assuming a shear coefficient derived from 40 m and 60 m AGL measurements. The comparisons for Tower 3 and Tower 6 (Figure 7 and Figure 8) indicate close agreement in the patterns on an annual, monthly and diurnal basis with a very moderate bias and spread of wind speed errors. The correlation on all time scales is certainly acceptable, with the hourly r^2 value of 0.525, the daily r^2 value of 0.79 and the monthly r^2 value of 0.892 for validation tower 3. This relationship exemplifies the model's ability to capture monthly and diurnal variations in the local climate.

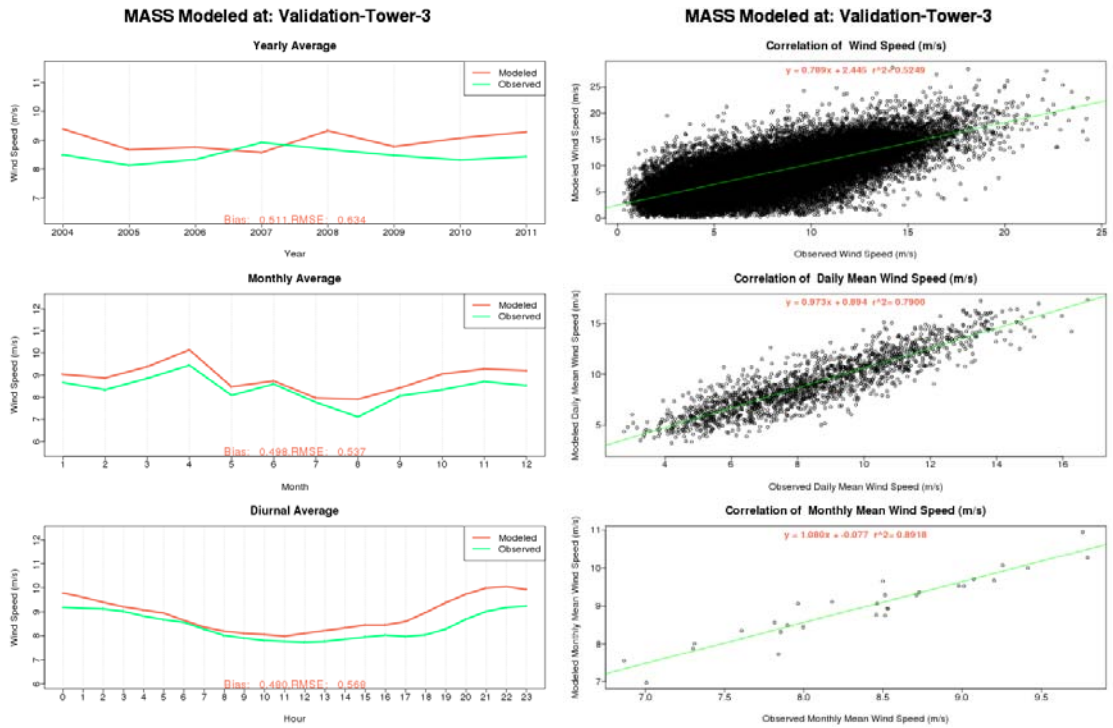

Figure 7. Comparison of simulated and observed mean wind speed on an annual, monthly and diurnal bias at validation tower 3. Hourly, daily and monthly scatter plot of observed vs. modeled showing the correlation between modeled and observed speeds.

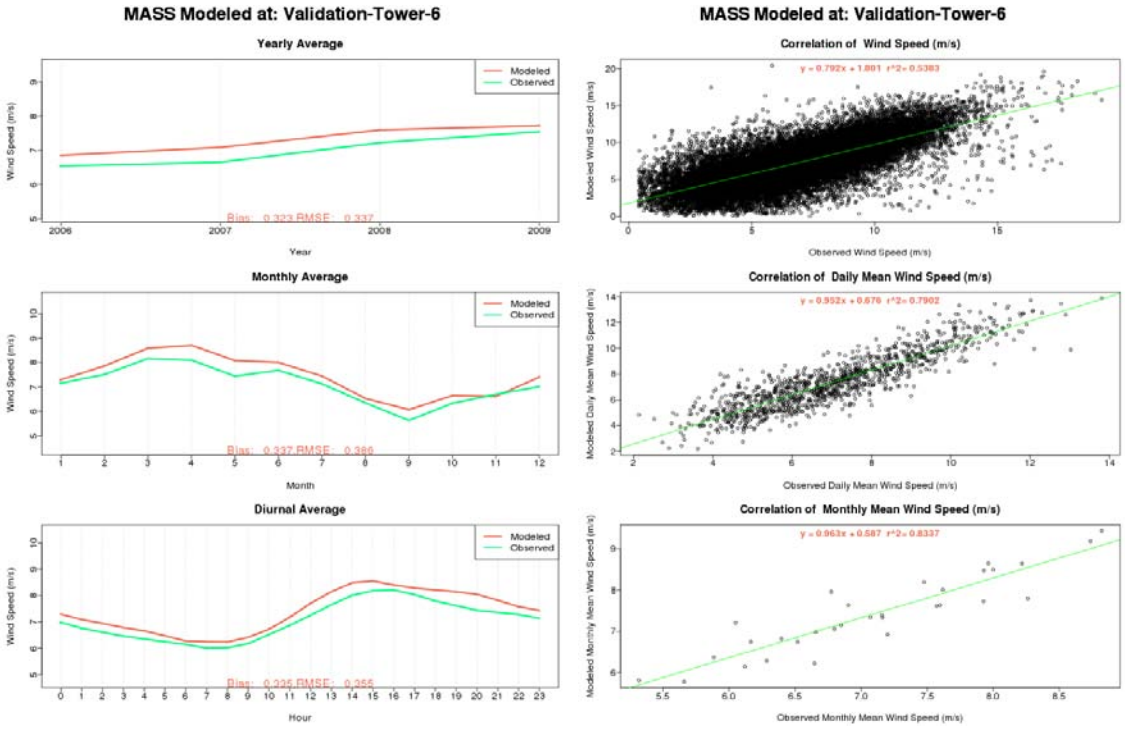

Figure 8. As in Figure 7 except for validation tower 6.

The wind power validation consisted of making direct comparisons with actual power generation data for ten power plants in the ERCOT region. In order to best characterize the difference between the modeled and observed power, these select number of sites were chosen based on preferable specifications detailed in the WFTI database, i.e. only power plants containing turbines with 80 m hub heights, known plant layouts and easily accessible power curve information were used for the analysis. The actual layouts were then modeled and compared against the power observations. Only the overlapping period of record was compared (generally 2005–2007), and times with unavailable generation data were set to missing in the modeled time series to facilitate a fair comparison.

The analysis shows that the model is able to capture the dynamic behavior of the wind plants in Texas quite well. The modeled seasonal and diurnal mean patterns are shown to be very similar to the observed but are biased slightly high, approximately 2.5% at Site 3 (Figure 9 and Figure 10). Some of the discrepancies may be caused by limitations in the numerical model or by a mean difference in the annual map speed while others are due to problems with wind plant performance (including availability and wind curtailment, see Figure 11). Overall the model is able to reproduce the increased power generation during nighttime hours when the height of the boundary layer is considerably lower and winds are stronger while predicting the seasonally dependent wind climate with acceptable accuracy.

Next the frequency distribution of hourly step changes in power output was compared to ensure that the model captures the variability of actual wind farms. Results at 3 ERCOT sites are shown in Figure 12. The changes are shown as a percentage of plant capacity, with the y-axis shown on a logarithmic scale to emphasize large ramps. The model variability compares well with the observed at each individual plant, as well as the aggregate of four wind power plants (Figure 12, bottom right). The aggregate ramp distribution demonstrates how geographic diversity and accumulating wind power generation tends to decrease the overall system fluctuation from hour to hour.

The correlation of hourly plant output was then compared at four of the power generation facilities. Approximately two years of hourly generation data was used to compute the linear regression coefficient (R) between each combination of plants. Figure 13 shows the correlation of Site 1 with each of the other locations. The results show that the model is slightly more correlated than the observed power, but still approximates the output well. The lower correlation in the observed data may also be attributed to wind curtailment or downtime at the facility. A similar comparison was done for the step change in power output. Additionally, the correlation coefficient was plotted against the distance between plants (Figure 14). It was found that the model tends to be slightly more correlated in space, but overall the modeled data exhibits realistic correlations when compared to the observed power data. Accurate spatial correlation is important because if output variations are highly correlated between projects, the benefit of geographic diversity is small, whereas little correlation between projects confers a large diversity benefit.

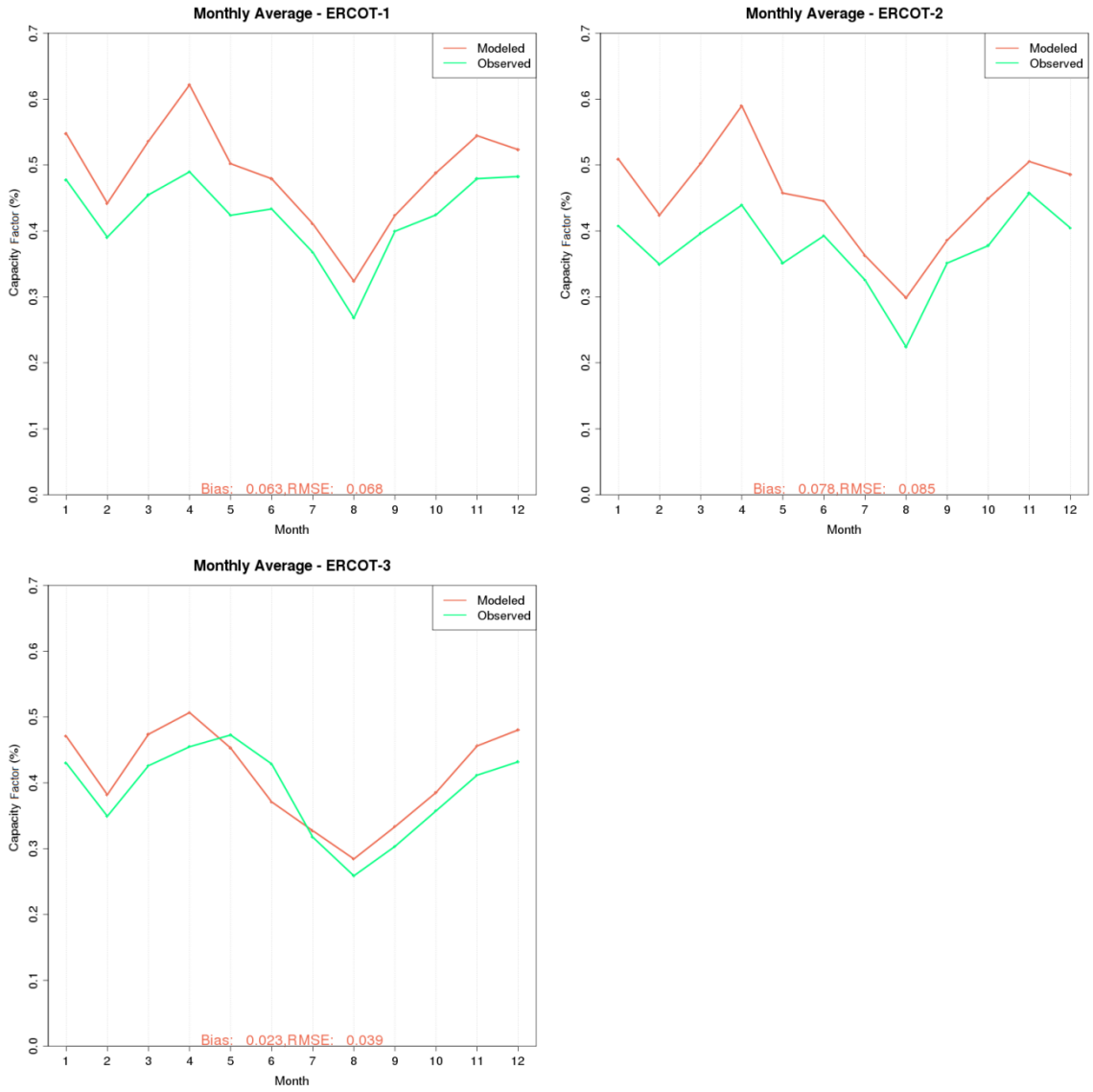

Figure 9. Comparison of monthly average capacity factors for three ERCOT power stations modeled at the nearest site.

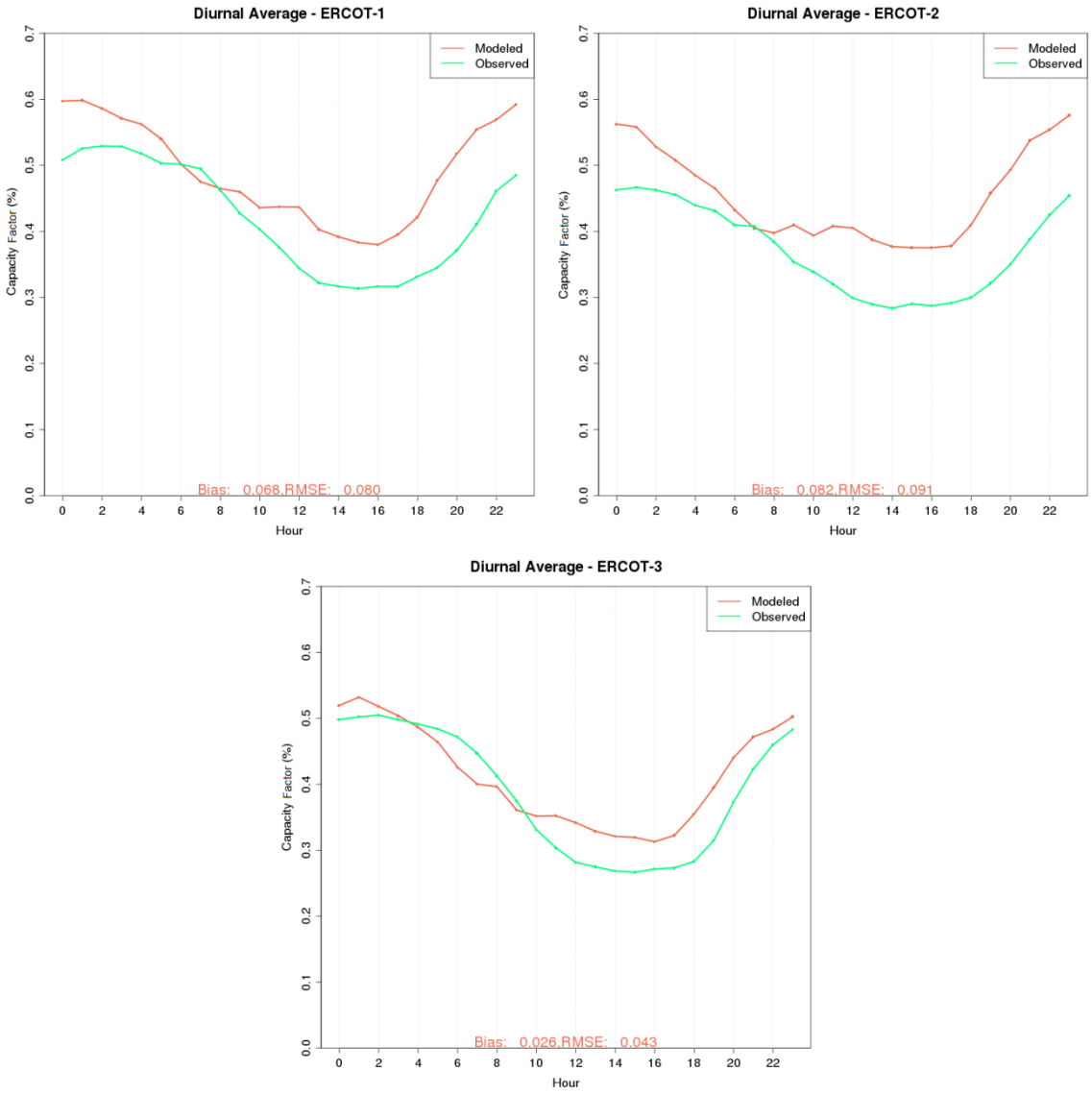

Figure 10. Comparison of diurnal average capacity factors for three ERCOT power stations modeled at the nearest site. Time is in Central Standard Time.

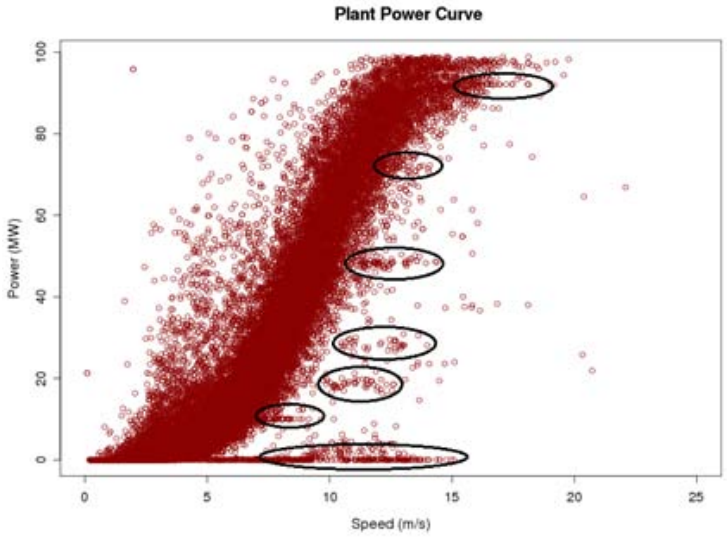

Figure 11. Example power output plotted as a function of wind speed with black ovals highlighting suspicious data points.

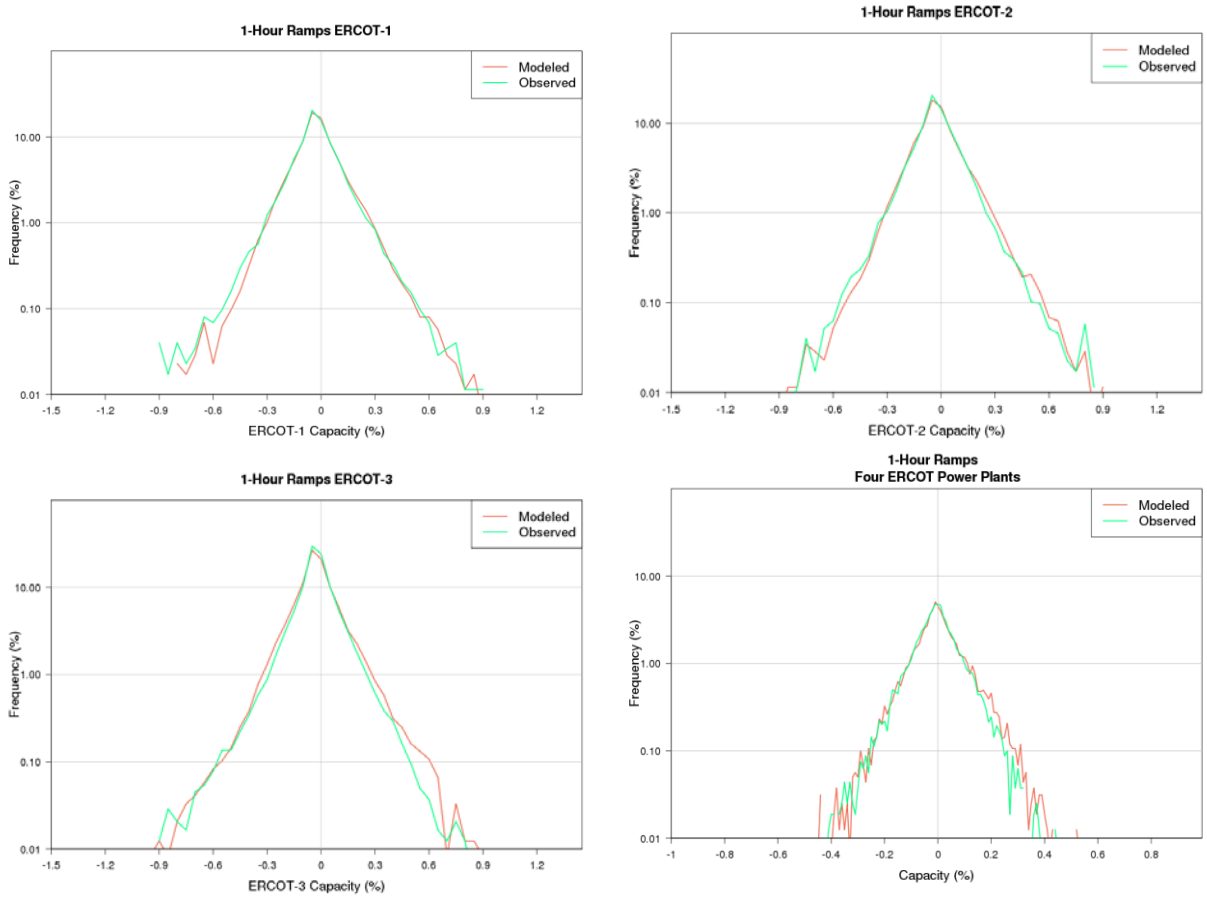

Figure 12. Comparison of 60-minute changes in power output on a logarithmic scale observed at three ERCOT stations as well as the aggregate of four ERCOT power generating facilities.

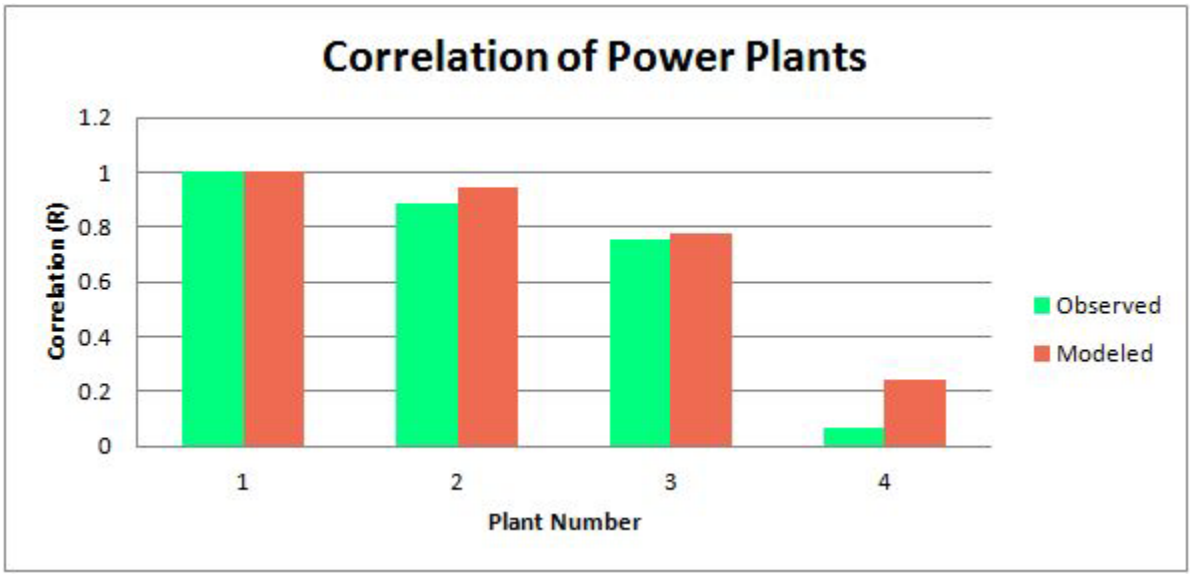

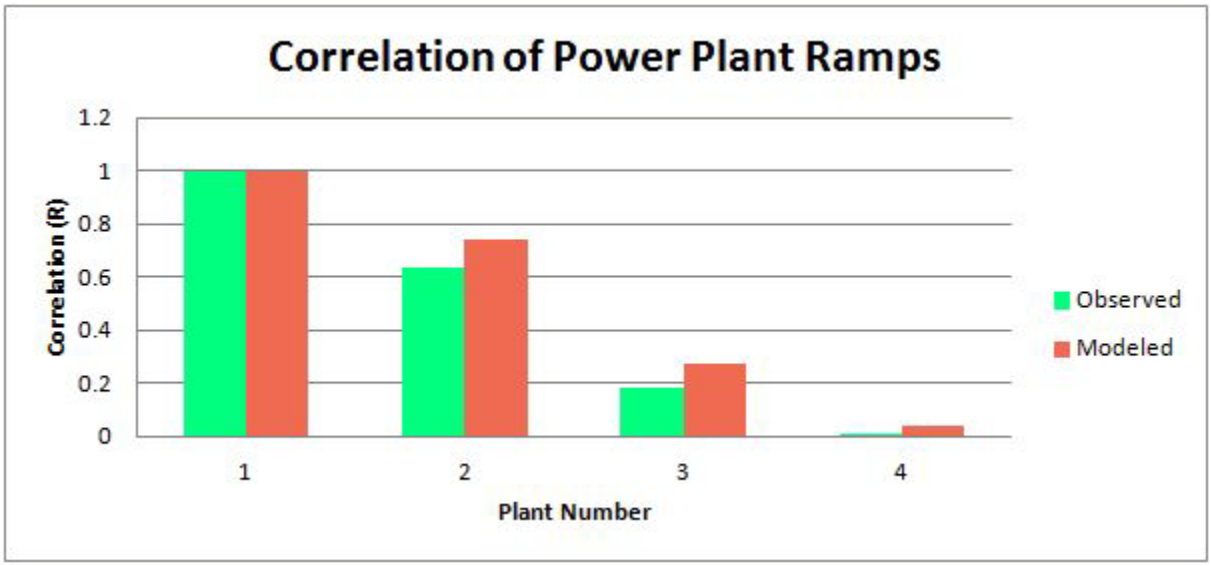

Figure 13. Correlation between modeled and observed power plants at four generating facilities. Shown for power generation and step change in power.

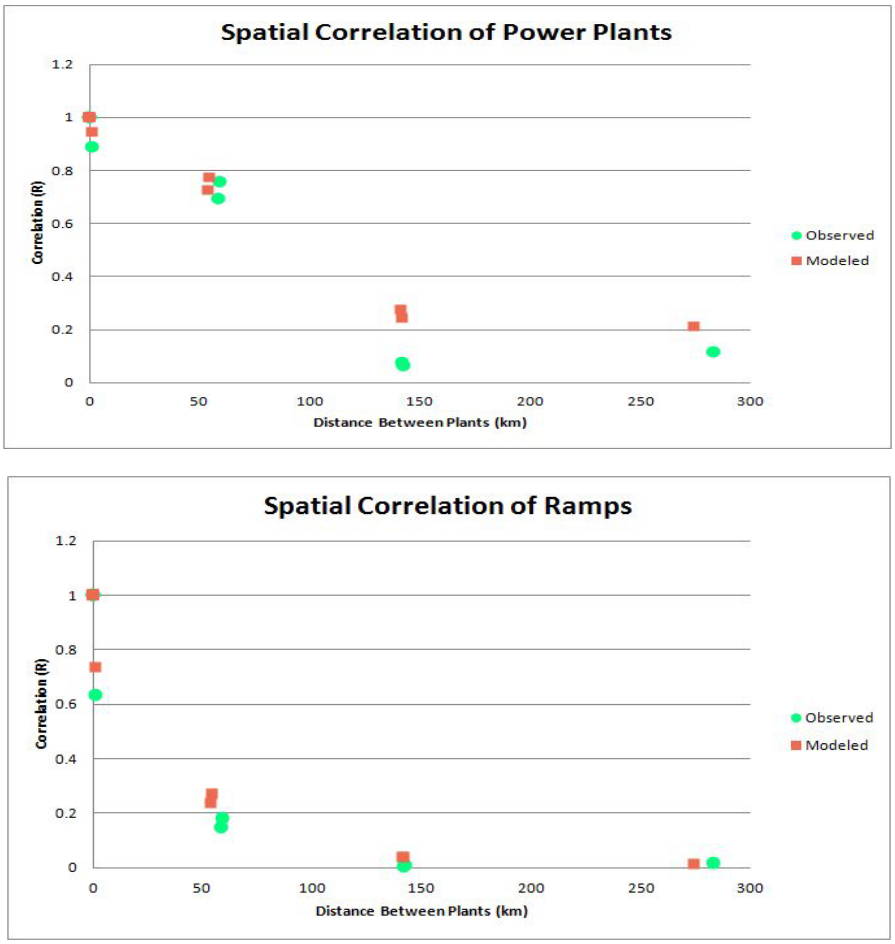

Figure 14. Spatial correlation of power plant output and step change in power at four generating facilities.

7. ACCURACY SUMMARY

Validation of modeled wind speeds against tall tower measurements and modeled power output against generation data at several existing plants was undertaken to ensure accuracy of the data set. Diurnal and monthly mean wind speeds validated well against observations at nearly all sites examined. Although some discrepancies were noted, diurnal and monthly mean modeled power output also compared with patterns observed at existing plants with acceptable accuracy. Comparison of hourly ramps in power output showed that the modeled data matches the variability observed at actual plants quite well.

It is not expected that the simulated wind and power profiles will exactly match the actual at a particular time or place. Some discrepancies may arise due to limitations in the numerical weather modeling, such as the finite grid resolution. Others may be caused by differences in assumed turbine model or wind plant performance (including low availability, curtailments, or outages).

No model is a perfect reflection of reality. However, the validation process confirmed that the data reflect realistic averages, seasonal and diurnal patterns, and ramping behavior of wind speed and power production for Texas wind farms, and should provide a solid basis for hourly grid impact simulations.

8. DATA SET USAGE

The data set was developed specifically for use in wind integration and transmission studies for the purpose of matching the relative changes in wind power output across time and space. It should be noted that modeled data is not a replacement for onsite measurements and should not be used as the only basis for investment decisions.

AWS Truepower maintains a secure offsite archive of the mesoscale model simulations performed for clients. Should the need arise for more wind plants or different technologies to be simulated in the ERCOT region, AWS Truepower can readily support these scenario building activities with 3 weeks of lead time (for offsite data retrieval and restoration).

9. CONCLUSIONS

AWST employed a numerical weather prediction model to simulate 15 years of hourly wind speeds and power output profiles for wind generation facilities across Texas. A site selection process identified existing, planned, and hypothetical wind generation facilities totaling over 29 GW onshore and 1.5 GW offshore. Power output profiles were developed for each site identified using common commercially available turbine power curves as of May 2012 and AWST's standard power conversion and loss estimation techniques. Wind speeds and power profiles were validated against available measurements and were found to capture the dynamic behavior of actual wind farms with acceptable accuracy. The data therefore appear to provide a sound basis for long-term system planning as well as transmission system and resource adequacy studies within the ERCOT region.

APPENDIX A: SELECTED SITES

SITE_ID	PLANT TYPE	LATITUDE	LONGITUDE	MW
1	Existing Sites	33.738	-97.359	112.5
2	Existing Sites	30.888	-102.486	77.2
3	Existing Sites	30.966	-102.366	82.5
4	Existing Sites	34.144	-101.109	59.8
5	Existing Sites	32.380	-100.630	126.5
6	Existing Sites	32.171	-100.205	169.5
7	Existing Sites	32.195	-101.854	123.6
8	Existing Sites	31.079	-102.114	74.9
9	Existing Sites	32.983	-101.233	84.0
10	Existing Sites	31.990	-101.120	199.5
11	Existing Sites	27.130	-97.461	100.8
12	Existing Sites	27.931	-97.451	179.9
13	Existing Sites	32.122	-101.385	58.8
14	Existing Sites	32.028	-102.816	152.6
15	Existing Sites	31.167	-100.611	150.0
16	Existing Sites	31.220	-102.145	40.3
17	Existing Sites	31.239	-102.236	79.3
18	Existing Sites	31.293	-102.188	79.3
19	Existing Sites	31.757	-104.772	39.8
20	Existing Sites	30.833	-102.345	150.0
21	Existing Sites	30.770	-102.446	150.0
22	Existing Sites	30.947	-102.212	82.5
23	Existing Sites	32.508	-100.581	197.0
24	Existing Sites	32.765	-99.460	165.6
25	Existing Sites	31.940	-100.790	69.6
26	Existing Sites	31.940	-100.790	80.0
27	Existing Sites	32.740	-100.730	63.0
28	Existing Sites	32.175	-101.401	121.9
29	Existing Sites	31.673	-104.742	28.5
30	Existing Sites	28.006	-97.270	200.1
31	Existing Sites	32.742	-100.826	120.0
32	Existing Sites	32.742	-100.826	130.5
33	Existing Sites	32.301	-100.043	114.0
34	Existing Sites	27.572	-98.911	150.0
35	Existing Sites	32.360	-100.213	232.5
36	Existing Sites	32.316	-100.189	120.6
37	Existing Sites	32.290	-100.120	170.2
38	Existing Sites	33.070	-98.360	120.0
39	Existing Sites	32.958	-101.614	89.0

40	Existing Sites	32.894	-101.598	91.0
41	Existing Sites	32.942	-101.305	66.0
42	Existing Sites	32.948	-101.144	99.0
43	Existing Sites	26.962	-97.570	138.5
44	Existing Sites	26.962	-97.570	138.5
45	Existing Sites	30.919	-102.108	84.0
46	Existing Sites	30.922	-102.156	76.5
47	Existing Sites	31.224	-102.251	79.3
48	Existing Sites	32.586	-99.538	200.0
49	Existing Sites	32.584	-99.540	100.0
50	Existing Sites	32.584	-99.540	100.0
51	Existing Sites	27.130	-97.530	160.8
52	Existing Sites	27.130	-97.530	100.8
53	Existing Sites	32.420	-100.215	150.0
54	Existing Sites	32.411	-100.129	101.2
55	Existing Sites	31.920	-100.970	112.5
56	Existing Sites	32.368	-100.329	149.5
57	Existing Sites	32.368	-100.329	214.5
58	Existing Sites	31.900	-100.820	186.0
59	Existing Sites	32.258	-100.327	223.5
60	Existing Sites	32.261	-100.126	213.0
61	Existing Sites	32.223	-100.138	115.0
62	Existing Sites	32.266	-100.105	184.0
63	Existing Sites	32.420	-100.680	124.5
64	Existing Sites	32.423	-100.675	126.0
65	Existing Sites	32.455	-100.722	25.5
66	Existing Sites	32.450	-100.720	24.0
67	Existing Sites	31.944	-101.246	90.0
68	Existing Sites	32.027	-101.362	124.2
69	Existing Sites	31.984	-101.437	142.5
70	Existing Sites	31.980	-101.440	115.5
71	Existing Sites	33.759	-100.994	150.0
72	Existing Sites	32.591	-100.674	249.0
73	Existing Sites	32.207	-101.388	30.4
74	Existing Sites	32.346	-100.409	16.0
75	Existing Sites	32.343	-100.337	37.5
76	Existing Sites	32.346	-100.409	97.5
77	Existing Sites	32.266	-100.417	129.0
78	Existing Sites	32.247	-100.499	105.8
79	Existing Sites	32.284	-100.598	119.0
80	Existing Sites	32.139	-100.311	80.5

81	Existing Sites	32.430	-100.640	209.0
82	Existing Sites	32.490	-98.470	60.0
83	Existing Sites	33.366	-98.700	117.5
84	Existing Sites	33.359	-98.650	107.5
85	Queue Sites	33.498	-98.566	50.0
86	Queue Sites	32.997	-100.528	30.0
87	Queue Sites	33.333	-99.493	400.0
88	Queue Sites	26.463	-97.678	206.0
89	Queue Sites	26.325	-97.641	400.0
90	Queue Sites	27.563	-98.871	92.0
91	Queue Sites	29.185	-100.199	100.0
92	Queue Sites	34.254	-99.438	170.0
93	Queue Sites	27.176	-97.586	202.0
94	Queue Sites	33.196	-98.364	150.0
95	Queue Sites	32.503	101.473	120.0
1006	Hypothetical Sites	34.509	-101.163	100.3
1009	Hypothetical Sites	31.051	-101.956	107.3
1014	Hypothetical Sites	34.520	-101.346	142.2
1017	Hypothetical Sites	31.074	-101.230	100.0
1022	Hypothetical Sites	34.646	-101.461	120.5
1024	Hypothetical Sites	31.040	-100.981	117.2
1025	Hypothetical Sites	30.698	-101.640	94.6
1026	Hypothetical Sites	31.762	-101.427	100.7
1028	Hypothetical Sites	31.036	-101.630	94.9
1029	Hypothetical Sites	33.756	-99.689	100.0
1030	Hypothetical Sites	33.245	-99.485	100.7
1031	Hypothetical Sites	31.874	-101.624	139.3
1032	Hypothetical Sites	34.488	-100.042	99.8
1033	Hypothetical Sites	31.058	-101.379	164.4
1036	Hypothetical Sites	31.963	-101.436	125.7
1037	Hypothetical Sites	33.392	-99.561	101.0
1039	Hypothetical Sites	33.039	-99.500	101.8
1040	Hypothetical Sites	30.632	-101.358	94.5
1041	Hypothetical Sites	33.220	-99.818	100.8
1042	Hypothetical Sites	34.504	-100.248	102.3
1043	Hypothetical Sites	33.671	-99.516	197.4
1050	Hypothetical Sites	34.407	-100.973	173.6
1053	Hypothetical Sites	34.547	-100.979	136.2
1054	Hypothetical Sites	34.720	-101.164	101.5
2013	Hypothetical Sites	34.607	-102.405	101.3
2014	Hypothetical Sites	34.738	-102.207	117.3

2016	Hypothetical Sites	34.586	-102.502	151.7
2018	Hypothetical Sites	34.611	-102.321	150.9
2019	Hypothetical Sites	34.739	-101.976	123.6
2021	Hypothetical Sites	34.512	-102.101	116.8
2022	Hypothetical Sites	33.806	-101.107	182.5
2026	Hypothetical Sites	34.737	-102.491	119.3
2027	Hypothetical Sites	34.716	-101.560	104.1
2028	Hypothetical Sites	34.742	-102.316	127.9
2029	Hypothetical Sites	34.502	-101.901	133.0
2030	Hypothetical Sites	34.443	-101.491	116.3
2031	Hypothetical Sites	34.444	-101.674	102.4
2032	Hypothetical Sites	34.488	-101.812	162.8
2033	Hypothetical Sites	34.698	-101.625	129.2
3001	Hypothetical Sites	35.613	-100.651	237.8
3002	Hypothetical Sites	35.601	-100.574	131.6
3003	Hypothetical Sites	35.581	-100.795	198.9
3004	Hypothetical Sites	35.379	-100.949	211.0
3005	Hypothetical Sites	35.559	-101.065	151.4
3006	Hypothetical Sites	35.611	-100.886	186.9
3007	Hypothetical Sites	35.411	-101.056	286.3
3008	Hypothetical Sites	35.370	-100.882	181.7
3009	Hypothetical Sites	35.194	-100.814	100.5
3011	Hypothetical Sites	34.587	-102.558	324.8
3014	Hypothetical Sites	34.715	-102.980	232.2
3015	Hypothetical Sites	34.595	-102.803	196.1
3017	Hypothetical Sites	34.731	-102.643	265.6
3018	Hypothetical Sites	34.727	-102.788	229.2
3019	Hypothetical Sites	34.666	-102.578	178.7
4001	Hypothetical Sites	35.484	-101.248	100.1
4002	Hypothetical Sites	35.539	-101.112	100.2
4003	Hypothetical Sites	34.185	-101.102	100.4
4004	Hypothetical Sites	35.425	-101.363	167.9
4005	Hypothetical Sites	35.449	-101.488	135.1
4006	Hypothetical Sites	34.267	-101.203	179.3
4007	Hypothetical Sites	32.953	-101.182	103.1
4011	Hypothetical Sites	34.280	-101.283	206.9
4014	Hypothetical Sites	33.559	-100.146	100.1
4015	Hypothetical Sites	34.299	-101.379	213.8
4016	Hypothetical Sites	32.928	-101.319	143.8
4017	Hypothetical Sites	33.752	-100.033	100.1
4018	Hypothetical Sites	34.289	-101.515	181.2

4019	Hypothetical Sites	32.897	-101.594	100.3
4021	Hypothetical Sites	33.791	-100.185	149.6
4025	Hypothetical Sites	32.930	-101.659	179.9
4026	Hypothetical Sites	32.533	-101.446	111.5
4030	Hypothetical Sites	34.273	-101.095	185.0
5002	Hypothetical Sites	26.254	-97.456	399.9
5003	Hypothetical Sites	26.293	-97.649	399.9
6001	Hypothetical Sites	32.101	-101.291	120.0
7001	Hypothetical Sites	29.531	-100.461	180.0
8001	Hypothetical Sites	31.672	-98.587	100.1
9001	Hypothetical Sites	35.663	-100.546	100.2
9003	Hypothetical Sites	35.793	-100.742	100.2
9012	Hypothetical Sites	30.518	-102.778	99.9
9018	Hypothetical Sites	30.811	-102.290	99.9
9023	Hypothetical Sites	30.519	-102.965	120.8
9027	Hypothetical Sites	35.875	-100.551	134.7
9035	Hypothetical Sites	34.871	-102.025	99.9
9038	Hypothetical Sites	35.238	-102.195	154.8
9043	Hypothetical Sites	33.680	-99.171	102.0
9045	Hypothetical Sites	34.936	-103.028	99.9
9047	Hypothetical Sites	32.352	-100.536	126.8
9048	Hypothetical Sites	34.973	-102.601	114.9
9049	Hypothetical Sites	34.931	-101.831	107.7
9051	Hypothetical Sites	35.299	-102.394	127.4
9053	Hypothetical Sites	30.485	-103.170	121.4
9059	Hypothetical Sites	35.089	-102.614	110.7
9063	Hypothetical Sites	35.109	-102.945	127.8
9064	Hypothetical Sites	30.816	-102.505	131.2
9065	Hypothetical Sites	35.239	-102.753	100.0
9071	Hypothetical Sites	34.972	-102.760	195.8
9075	Hypothetical Sites	31.063	-100.927	119.4
9077	Hypothetical Sites	31.881	-98.733	104.4
9080	Hypothetical Sites	33.460	-98.861	100.0
9100	Hypothetical Sites	34.100	-99.009	127.5
9111	Hypothetical Sites	33.872	-99.097	138.6
9120	Hypothetical Sites	31.286	-102.268	120.7
9130	Hypothetical Sites	33.652	-98.279	100.1
9155	Hypothetical Sites	27.223	-97.438	100.1
9161	Hypothetical Sites	33.148	-98.085	99.9
9162	Hypothetical Sites	31.622	-98.436	160.2
9168	Hypothetical Sites	29.933	-100.789	99.9

9192	Hypothetical Sites	26.711	-97.474	122.9
9199	Hypothetical Sites	33.035	-100.533	134.9
9208	Hypothetical Sites	31.292	-101.830	157.0
9216	Hypothetical Sites	29.749	-101.237	103.0
9217	Hypothetical Sites	27.334	-98.987	100.0
9237	Hypothetical Sites	27.502	-97.348	100.0
9238	Hypothetical Sites	33.206	-98.302	128.9
9244	Hypothetical Sites	33.116	-100.317	132.9
9297	Hypothetical Sites	31.846	-98.558	172.4
9303	Hypothetical Sites	27.525	-97.659	100.1
9311	Hypothetical Sites	27.955	-97.287	100.4
9334	Hypothetical Sites	26.924	-98.867	110.8
9342	Hypothetical Sites	26.541	-97.612	100.0
9360	Hypothetical Sites	27.990	-97.441	120.1
9408	Hypothetical Sites	26.404	-97.860	100.5
9411	Hypothetical Sites	26.232	-97.907	100.5
9419	Hypothetical Sites	28.049	-97.715	100.0
9441	Hypothetical Sites	26.258	-98.065	100.1
9471	Hypothetical Sites	26.539	-97.759	163.8
9489	Hypothetical Sites	26.569	-97.911	135.3
9518	Hypothetical Sites	28.334	-98.264	99.9
9592	Hypothetical Sites	29.884	-97.487	100.1
20001	Offshore	29.098	-94.866	500.0
20002	Offshore	27.608	-97.012	500.0
20003	Offshore	26.230	-97.053	500.0